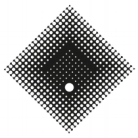
VICTORIA UNIVERSITY
MELBOURNE AUSTRALIA

Local buckling of steel plates in concrete-filled steel tubular columns at elevated temperatures

This is the Accepted version of the following publication

Kamil, Ghanim Mohammed, Liang, Qing and Hadi, Muhammad NS (2018) Local buckling of steel plates in concrete-filled steel tubular columns at elevated temperatures. Engineering Structures, 168. 108 - 118. ISSN 0141-0296

The publisher's official version can be found at https://www.sciencedirect.com/science/article/pii/S0141029617334739
Note that access to this version may require subscription.

Downloaded from VU Research Repository https://vuir.vu.edu.au/37141/

Kamil, G. M., Liang, Q. Q. and Hadi, M. N. S. (2018). Local buckling of steel plates in concrete-filled steel tubular columns at elevated temperatures. *Engineering Structures*, 168: 108-118

Local buckling of steel plates in concrete-filled steel tubular columns at elevated temperatures

Ghanim Mohammed Kamil[a], Qing Quan Liang[a,*], Muhammad N. S. Hadi[b]

[a] *College of Engineering and Science, Victoria University, PO Box 14428, Melbourne, VIC 8001, Australia*

[b] *School of Civil, Mining and Environmental Engineering, University of Wollongong, Wollongong, NSW 2522, Australia*

Abstract

Local buckling remarkably reduces the strength of steel plates in rectangular thin-walled concrete-filled steel tubular (CFST) columns at ambient temperature. This effect is more remarkable at elevated temperature. However, there have been very limited experimental and numerical investigations on the local and post-local buckling behavior of steel plates in CFST columns at elevated temperatures. This paper presents numerical studies on the local and post-local buckling behavior of thin steel plates under stress gradients in rectangular CFST columns at elevated temperatures. For this purpose, finite element models are developed, accounting for geometric and material nonlinearities at elevated temperatures. The initial geometric imperfections and residual stresses presented in steel plates are considered. Based on the finite element results, new formulas are proposed for determining the initial local buckling stress and post-local buckling strength of clamped steel plates under in-plane stress gradients at elevated temperatures. Moreover, new effective width formulas are developed for clamped steel plates at elevated temperatures. The proposed formulas are compared with existing ones with a good agreement. The effective width formulas developed are used in the calculations of the ultimate axial loads of rectangular CFST short columns exposed to fire and the results obtained are

* Corresponding author. Tel.: 61 3 9919 4134.
E-mail address: Qing.Liang@vu.edu.au (Q. Q. Liang)

compared well with the finite element solutions provided by other researchers. The initial local buckling and effective width formulas can be implemented in numerical techniques to account for local buckling effects on the responses of rectangular thin-walled CFST columns at elevated temperatures.

Keywords: Concrete-filled steel tubes; Effective width; Elevated temperatures; Finite element analysis; Local buckling; Post-local buckling

1. Introduction

Filling concrete into a rectangular thin-walled steel tubular column as shown in Fig. 1 results in a significant increase in its ultimate strength and fire resistance as reported by Schneider [1], Sakino et al. [2], Liang et al. [3] and Dundu [4]. However, the thin steel tube walls of a rectangular concrete-filled steel tubular (CFST) column under applied loads may undergo outward local buckling, which remarkably reduces the strength of the column as discussed by Liang [5]. In a fire condition, the strength and stiffness of steel plates decrease significantly with an increase in the elevated temperature [6, 7]. As a result, the local buckling of thin steel plates at elevated temperatures is more likely to occur than the ones at ambient temperatures. In addition, the local and post-local buckling strengths of a thin steel plate at elevated temperature are much lower than those of the plate at ambient temperature. It is assumed that the steel tube walls of a rectangular CFST column under axial load and bending have a clamped boundary condition that recognizes the restraint provided by the rigid concrete core and are subjected to in-plane stress gradients [5]. The CFST columns have been widely used in high-rise composite buildings that could be exposed to fire. The behavior of CFST columns at elevated temperatures has been investigated by researchers [8-11]. However, little attention has

been devoted to the study of the local and post-local buckling problem of clamped steel plates under stress gradients in CFST columns at elevated temperatures. Therefore, this paper addresses this challenging problem.

The local and post-local buckling behavior of steel plates under edge stresses at ambient temperature has been investigated by many researchers [12-17]. Shanmugam et al. [16] presented an analytical study on the post-local buckling strengths of steel plates in thin-walled steel box columns under biaxial loads. The steel plates of the hollow steel box column were assumed to be simply-supported. Effective width expressions were proposed by Shanmugam et al. [16] for calculating the post-local buckling strengths of simply-supported steel plates under stress gradients. Uy and Bradford [18] and Uy [19] conducted experiments to examine the local buckling characteristics of thin steel plates in rectangular CFST columns. Liang et al. [20] developed nonlinear finite element models to study the critical local and post-local buckling strengths of steel plates in biaxially loaded CFST columns where the steel tube walls could be subjected to stress gradients. They proposed design formulas for computing the critical local and post-local buckling strengths of clamped steel plates under stress gradients. Moreover, effective width formulas were developed by Liang et al. [20] and implemented in numerical models by Liang [21, 22] to account for local buckling effects on the strength and ductility of rectangular CFST columns

Thin steel plates at elevated temperatures are more susceptible to local buckling because the elevated temperatures significantly reduce their stiffness and strength [7, 23]. Heidarpour and Bradford [24] used a spline finite strip method of buckling analysis to investigate the local buckling of flange outstands subjected to elevated temperatures and proposed the plasticity and yield slenderness limits. The local buckling temperatures of plates under certain boundary

conditions were also anticipated. Knoblock [7] investigated the local buckling behavior of steel sections at elevated temperatures. He suggested that the methods commonly used for calculating the strength of steel sections and for section classification subjected to elevated temperatures should be revised. Couto et al. [25] used a finite element analysis software to study the local buckling of simply-supported steel plates at elevated temperatures. These steel plates were subjected to in-plane bending or compressive edge stresses. The residual stress pattern at ambient temperatures was assumed for the plates at elevated temperatures. A constant initial geometric imperfection at the plate centre was considered regardless of the plate thickness. Design formulas were proposed for determining the ultimate strength of simply-supported plates at elevated temperatures. Quiel and Garlock [26] utilized the computer program SAFIR to determine the local buckling strengths of steel plates exposed to fire. The loaded edges of the steel plate were assumed to be simply-supported while the unloaded edges were either simply-supported or fixed. However, the effect of residual stresses was not considered in their study. They proposed expressions for estimating the ultimate strengths of steel plates with various boundary conditions.

However, none of the studies reported in the literature investigated the local and post-local buckling behavior of clamped steel plates under stress gradients in CFST columns at elevated temperatures. There is a lack of effective width formulas for steel plates that could be incorporated in numerical models to account for local buckling effects on the strength of rectangular thin-walled CFST columns at elevated temperatures. Therefore, to bridge the knowledge gap, this paper utilizes the finite element program ANSYS 16 [27] to study the local and post-local buckling behavior of clamped steel plates under stress gradients in rectangular CFST columns at elevated temperatures. The effects of residual stresses and initial geometric imperfections presented in the steel plates are taken into account. Based on the results obtained

from the nonlinear finite element analyses, design formulas are proposed for determining the initial local and post-local buckling strengths of clamped steel plates under stress gradients at elevated temperatures and verified by comparisons with the ones proposed by other researchers and with finite element results on rectangular CFST short columns at elevated temperatures.

2. Nonlinear finite element analysis of plates

2.1. General

The finite element analysis program ANSYS 16 [27] was employed in the present study to investigate the critical local and post-local buckling strengths of steel plates in CFST columns at elevated temperatures. The steel tube walls of a rectangular CFST column under compression can only buckle locally outward due to the restraint provided by the concrete core. This restraint effect was considered in the finite element model by incorporating an initial geometric imperfection caused by the lateral pressure applied on the plate. This implies that the steel plate can only buckle locally outward in the nonlinear analysis. The local and post-local buckling of steel plates in CFST columns at ambient temperatures has been studied by Liang et al. [20] and the effective width formulas proposed by them have been incorporated in the fiber element models to accurately account for local buckling effects on the behavior of CFST columns by Liang [21,22]. As suggested by Liang et al. [20], the four edges of the steel tube wall were treated as clamped due to the restraint provided by the rigid concrete core. The boundary conditions of the clamped plate are schematically depicted in Fig. 2. A square steel plate was chosen to simulate the webs and flanges of a CFST column at elevated temperatures. The von Mises yield criterion was used in the material models to treat the material plasticity. The four-node shell/plate element SHELL 181 in ANSYS 16 was used to discretize the steel plate into a

20×20 mesh. The sensitivity analysis of the element size was conducted and the results obtained are shown in Fig. 3, which indicates that the 20×20 mesh is suitable in terms of the computational time and the accuracy of the results.

2.2. Applied edge stresses on steel plates

The two adjacent steel tube walls of a rectangular CFST columns under axial load and biaxial bending may be subjected to non-uniform compressive stresses while the other two adjacent walls are under in-plane bending stresses as discussed by Liang et al. [20], Liang [21,22] and Liang [5]. Figure 2 illustrates a steel plate under non-uniform edge compressive stresses. For a rectangular CFST column under axial compression, its four steel tube walls are subjected to uniform compressive stresses. The top flange of the CFST column under uniaxial bending is in uniform compression while other steel tube walls are subjected to either tension or in-plane bending stresses. The stress gradient coefficient is used to define the stress ratio of the non-uniform compressive stresses on the steel plate. The stress gradient is maintained by the applied edge stresses on the plate as shown in Fig. 2. Only steel plates under compressive edge stresses are considered in the present study.

2.3. Geometric imperfections

The initial geometric imperfections have a significant effect on the local buckling of thin steel plates. Feng et al. [28] conducted numerical analyses to examine the effect of initial geometric imperfections on the ultimate strengths of rectangular cold-formed hollow steel columns exposed to uniform elevated temperatures. They concluded that the magnitude of the initial imperfection had a remarkable effect on the strength of the hollow steel columns. Liang et al.

[20] used an initial geometric imperfection of $0.1t$ (where t is the plate thickness) at the plate center in the nonlinear local and post-local buckling analyses of steel plates at ambient temperatures. Quiel and Garlock [26] examined the effects of initial geometric imperfections of $0.1t$ and $b/200$ (where b is the plate width) on the buckling strengths of steel plates at elevated temperatures. The numerical results obtained indicated that there were not much differences between the buckling strengths predicted using these two initial geometric imperfections. Couto et al. [25] considered an initial geometric imperfection of 80% *b/t* for the steel plates in their models. In the present study, the initial geometric imperfection at the plate center was taken as $0.1t$. A lateral uniform pressure was applied to the plate to induce the required initial geometric imperfection. The value of the lateral pressure was determined by a trial-and-error method and by conducting a nonlinear analysis on the plate until the $0.1t$ deflection at the plate centre was obtained.

2.4. Residual stresses

The residual stress pattern depicted in Fig. 4 was applied to the steel plate as suggested by Liang et al. [20] and Abambres and Quach [29]. The tensile residual stresses were presented at the welds while the rest of the plate was subjected to the compressive residual stresses. The compressive residual stress was taken as 25% of the steel yield strength. In the finite element model, the residual stresses were applied to the steel plate by prestresses. Research studies indicated that the residual stresses locked in the steel plate were released at a temperature above 400°C [30-34]. Therefore, the residual stresses were not considered for steel plates at temperatures above 400°C in the present study.

2.5. Stress-strain relationships for steels at elevated temperatures

The stress-strain relationships given in Eurocode 3 [35] were adopted in the finite element model to simulate the material behavior of steel plates at elevated temperatures. Figure 5 depicts the stress-strain curve for structural steels without strain hardening at elevated temperatures, which is expressed by

$$\sigma_T = \begin{cases} E_T\ \varepsilon_T & \text{for } \varepsilon_T \le \varepsilon_{p,T} \\ (f_{p,T} - h_3) + \dfrac{h_2}{h_1}\sqrt{h_1^{\,2} - (\varepsilon_{y,T} - \varepsilon_T)^2} & \text{for } \varepsilon_{p,T} \le \varepsilon_T \le \varepsilon_{y,T} \\ f_{y,T} & \text{for } \varepsilon_{y,T} \le \varepsilon_T \le \varepsilon_{u,T} \end{cases} \quad (1)$$

where

$$h_1^{\,2} = (\varepsilon_{y,T} - \varepsilon_{p,T})(\varepsilon_{y,T} - \varepsilon_{p,T} + h_3 / E_T) \quad (2)$$

$$h_2^{\,2} = E_T(\varepsilon_{y,T} - \varepsilon_{p,T})h_3 + h_3^{\,2} \quad (3)$$

$$h_3 = \frac{(f_{y,T} - f_{p,T})^2}{E_T(\varepsilon_{y,T} - \varepsilon_{p,T}) - 2(f_{y,T} - f_{p,T})} \quad (4)$$

where E_T is the elastic modulus of steel, $f_{p,T}$ is the proportional limit, $f_{y,T}$ is the effective yield strength, $\varepsilon_{p,T}$ is the strain corresponding to $f_{p,T}$, $\varepsilon_{y,T}$ is the yield strain, and $\varepsilon_{u,T}$ is the ultimate strain at elevated temperatures.

The strain hardening is considered for structural steels at temperatures less than 300^{o}C using the following equation [35]:

$$\sigma_T = [(f_{u,T} - f_{y,T})/0.02]\,\varepsilon_T - f_{u,T} + 2\,f_{y,T} \qquad \text{for } 0.02 < \varepsilon_T < 0.04 \tag{5}$$

For $\varepsilon_T \geq 0.04$, σ_T equals to the ultimate tensile strength of the steel at elevated temperature.

Elevated temperatures significantly reduce the material properties of structural steels. The reduction factors applied to the material properties of structural steels at elevated temperatures given in Eurocode 3 [35] are shown in Fig. 6, where $k_{p,T}$ is the reduction factor of the proportional limit, $k_{y,T}$ is the reduction factor of the yield strength, $k_{0.2p,T}$ is the reduction factor of the proof stress, $k_{E,T}$ is the reduction factor of the Young's modulus, $k_{u,T}$ is the reduction factor of the ultimate tensile strength.

2.6. Verification of the finite element model

Before utilizing the finite element model to investigate the local and post-local buckling behavior of steel plates at elevated temperatures, comparisons have been made to verify the finite element model at both ambient and elevated temperatures. A rectangular simply-supported steel plate with an initial imperfection of $0.1t$ at ambient temperature reported by Quiel and Garlock [26] was analysed. The ultimate strength curve of the steel plate obtained by the finite element analysis is compared with that given by Quiel and Garlock [26] in Fig. 7. The figure shows that a good agreement between these two solutions is obtained. A nonlinear finite element analysis on a simply-supported rectangular steel plate with a/b ratio of 5 (where a is the plate length) and initial geometric imperfection of $0.1t$ and no residual stresses at an elevated temperature of 700^{o}C was performed. It can be seen from Fig. 8 that the finite element

model predicts well the performance of the steel plates with various slenderness ratios at elevated temperature.

3. Post-local buckling behavior at elevated temperatures

The nonlinear finite element model developed was employed to investigate the local and post-local behavior of clamped steel plates at temperatures ranging from 20 to $700^{o}C$ and subjected to in-plane stress gradients as shown in Fig. 2. Four temperature levels were considered in addition to the ambient temperature, which were 200, 400, 600, and $700^{o}C$. The square steel plates of 500×500 mm with initial geometric imperfections of $0.1t$ and *b/t* ratios ranging from 30 to 110 with an increment of 10 were considered. The stress gradient coefficient (α) is defined as the ratio of the minimum edge stress to the maximum edge stress. The stress gradient coefficient (α) varied from 0.0 to 1.0 with an increment of 0.2. The yield strength of steel plates at ambient temperature was 300 MPa and the Young's modulus was 210 GPa. At elevated temperatures, the reduction coefficients for the material properties given in Eurocode 3 [35] were used. The typical local and post-local buckling modes of steel plates under uniform edge compressive stresses at elevated temperatures are shown in Fig. 9.

Figures 10 and 11 show the load-lateral deflection curves for the steel plate with a *b/t* ratio of 70 subjected to stress gradients at ambient temperature and 600°C, respectively. It appears that the post-local buckling strength or the ultimate strength of the steel plate decreases with an increase in the stress gradient coefficient α regardless of the temperature levels. However, for the plate under the same stress gradient, increasing the temperature significantly reduces its post-local buckling strength. It can be observed from Figs. 10 and 11 that at both temperature levels, the steel plate under uniform edge stresses ($\alpha = 1.0$) could not attain its yield strength

due to the effects of initial geometric imperfection, residual stresses and the deterioration of material properties at elevated temperatures. When the stress gradient coefficient is small and the temperature is low, the post-local buckling strength of the steel plate with a small *b/t* ratio may be higher than its yield strength. This is attributed to the strain hardening of the steel material as reported by Usami [14, 15] and Liang et al. [20].

Figure12 shows load-lateral deflection curves for steel plates with $b/t = 80$ subjected to uniform edge stresses at different temperatures. It can be seen from the figure that the post-local buckling strength of steel plates decreases significantly with an increase in the temperature level. Moreover, increasing the temperature remarkably reduces the flexural stiffness of the steel plate. The ultimate strength curves of steel plates at ambient temperature and temperatures of 200°C, 400°C, 600°C and 700°C are shown in Figs. 13-17, respectively. It appears that the post-local buckling strength of clamped steel plates generally decreases with increasing their slenderness ratios regardless of the temperature levels and stress gradients. Under the same temperature level, increasing the stress gradient coefficient significantly reduces the post-local buckling strength of the steel plate. Furthermore, for a steel plate with the certain *b/t* ratio and stress gradient, its post-local buckling strength is shown to be reduced by increasing the temperature. When the temperature level increases from 20°C to 700°C, the ultimate strength of steel plates decreases from $0.804f_y$ to $0.55f_{y,T}$.

4. Critical local buckling strengths at elevated temperatures

As shown in Figs. 10-12, it is obvious that there is no way to determine the initial local buckling stress of a steel plate because of geometric imperfections. The method presented by Liang et al. [20] was utilized to predict the initial local buckling stress of steel plates with imperfections. In

this method, the non-dimensional central lateral deflection versus the ratio of the deflection to the applied load is plotted as shown in Figs. 18 and 19 for steel plates with a *b/t* ratio of 100 at ambient temperature and at 600°C, respectively. The minimum value on the curve represents the onset of the critical local buckling of the plate. It can be observed from Figs. 18 and 19 that the general trend of the curves is that the w/σ_1 ratio of the plate decreases with an increase in its lateral deflection at the plate center. This is because the lateral deflection of the plate at the initial loading stages is small before initial local buckling. After reaching the minimum, however, the w/σ_1 ratio increases significantly with increasing the lateral deflection. This is attributed to the fact that after the onset of the plate local buckling, the plate undergoes large deflections under the load increments. It appears that the minimum w/σ_1 ratio indicates the onset of local buckling. For a steel plate under the same stress gradient and lateral deflection, the w/σ_1 ratio at elevated temperature is higher than that at ambient temperature. This means that at the same deflection the critical local buckling stress of the plate decreases with increasing the temperature level. This is reasonable because increasing the temperature reduces the material properties and strength.

The critical local buckling strengths of steel plates subjected to various temperature levels as a function of the relative slenderness ratio are given in Figs. 20-24. It appears that the reduction in strength at any level of temperature increases with increasing the *b/t* ratio and stress gradient coefficient. The numerical results presented show that the elevated temperature significantly reduces the criterial local buckling stress of steel plates. The local buckling strength of steel plates at the ambient temperature with a b/t ratio of 60 subjected to uniform edge stress is about $0.61f_y$, while at a temperature of 600°C is about $0.181f_{y,T}$. As illustrated in Figs. 20-24, the stress gradient ratio has a significant effect on the critical buckling strength of plates

especially at higher temperatures. The critical buckling strength decreases with increasing the stress gradient ratio.

5. Proposed design formulas

5.1. Design formulas for critical local buckling strengths

The factors that affect the local buckling behavior of clamped steel plates with an initial imperfection of $0.1t$ and residual stresses include the b/t ratio, stress gradient coefficient (α), and the yield strength of steel plate at ambient and elevated temperatures. It is worth to mention that the *b/t* ratio has been replaced with the non-dimensional slenderness ratio $\left(\lambda_{c,T}\right)$ for comparison purposes. Based on the results obtained from the nonlinear finite analyses, design formulas for determining the critical local buckling strengths of clamped steel plates under stress gradients have been proposed and presented herein.

For steel plates at temperature of 600°C, the critical local buckling stresses of the plates is proposed as:

$$\frac{\sigma_{lc,T}}{f_{y,T}} = \left(0.1916\lambda_{c,T}^{-0.7661} + 0.003889\right)\left(m_1\lambda_{c,T}^2 + m_2\lambda_{c,T} + m_3\right) \quad (6)$$

where $\sigma_{lc,T}$ is the critical local buckling strength of the steel plate at elevated temperatures, and $\lambda_{c,T}$ is the plate slenderness ratio at elevated temperature, which is expressed by

$$\lambda_{c,T} = \sqrt{\frac{12(1-\nu^2)(b/t)^2(k_{y,T}f_y)}{k\pi^2(k_{E,T}E)}} \tag{7}$$

in which ν is the Poisson's ratio, f_y is the steel yield strength at ambient temperature, $k = 9.95$ is the elastic local buckling coefficient and E is the Young's modulus of steel material at ambient temperature.

The coefficients m_1, m_2 and m_3 in Eq. (6) are given as

$$m_1 = -1.0685\alpha^2 + 2.275\alpha - 0.8969 \tag{8}$$

$$m_2 = 2.3075\alpha^2 - 4.7791\alpha + 1.8475 \tag{9}$$

$$m_3 = -0.825\alpha^2 + 1.086\alpha + 1.0083 \tag{10}$$

For any other temperatures, the critical local buckling stress of steel plates is proposed as

$$\frac{\sigma_{1c,T}}{f_{y,T}} = (g_1\lambda_{c,T}^{g} + g_2)\frac{0.6566\lambda_{c,T}^{0.001521}\left(\frac{k_{p,T}}{k_{y,T}}\right)^{-0.1598}}{0.5415\lambda_{c,T}^{4.889} + \left(\frac{k_{p,T}}{k_{y,T}}\right)^{-0.8252}} \tag{11}$$

where the coefficients g, g_1 and g_2 are

$$g = -7.9339\alpha^2 + 11.29\alpha + 4.701 \tag{12}$$

$$g_1 = 0.0863\alpha^2 - 0.1248\alpha + 0.0431 \tag{13}$$

$$g_2 = 0.2656\alpha^2 - 0.9902\alpha + 1.719 \tag{14}$$

The critical buckling strengths of thin steel plates under stress gradients at various temperatures calculated using the proposed formulas are compared with those obtained from the nonlinear finite element analyses in Figs. 20-24. It can be observed that good agreement between these two solutions is obtained.

5.2. Design formulas for post-local buckling strengths

The post-local buckling strength of thin steel plates depends on the plate slenderness ratio ($\lambda_{c,T}$), the stress gradient coefficient (α) and the level of temperature. Based on the results obtained from the finite element analyses, the design formula for determining the post-local buckling strengths of clamped thin steel plates in CFST columns is proposed as

$$\frac{\sigma_{1u,T}}{f_{y,T}} = (q_1\lambda_{c,T}^{q})\frac{0.8418\lambda_{c,T}^{0.02368}\left(\frac{k_{p,T}}{k_{y,T}}\right)^{-0.3028} + 1.154\left(\frac{k_{p,T}}{k_{y,T}}\right)}{2.055 + \lambda_{c,T}^{1.68}} \tag{15}$$

where $\sigma_{1u,T} \le 1.25 f_y$ for temperature less than 300°C and q and q_1 are written as

$$q = 0.04007\alpha^2 - 0.05275\alpha + 0.03355 \tag{16}$$

$$q_1 = 0.1007\alpha^2 - 0.7027\alpha + 1.65 \tag{17}$$

The post-local buckling strengths of thin steel plates under stress gradients at various temperatures computed by using Eq. (15) are compared with those obtained from the nonlinear

post-local buckling analyses in Figs. 13-17. The figures demonstrate that the proposed formula yields good predations of the finite element results.

5.3 Effective width formulas

The effective width concept [36] is used to describe the post-local buckling behavior of thin steel plates in Eurocode 3 [35] and AISC [37] as illustrated in Fig. 25. In Eurocode 3, the effective width of steel plates at elevated temperatures is taken as that of the plates at ambient temperatures using the proof stress. Reduction factors are applied to the material properties due to high temperature effects. The AISC [37] uses a similar effective width approach to calculate the buckling strength of steel plates at elevated temperatures. The effective width formulas have been proposed for estimating the post-local buckling strengths of thin steel plates under different boundary conditions at ambient and elevated temperatures by various researchers. Liang et al. [20] proposed effective width formulas for clamped steel plates under stress gradients at ambient temperature. Quiel and Garlock [26] developed equations for computing the effective widths of steel plates under thermal loading where the two loaded edges were simply-supported. Couto et al. [25] presented an expression for determining the ultimate strengths of simply-supported steel plates at elevated temperatures. Effective width formulas can be implemented in the nonlinear analysis procedures to account for local buckling effects on the behavior of rectangular thin-walled CFST columns [21, 22].

Based on the results obtained from the finite element analyses, the effective width formulas for clamped steel plate under stress gradients at any temperatures are proposed as follows:

$$\frac{b_{e1}}{b}=\frac{1}{2}(q_1\lambda_{c,T}^{q})\frac{0.8418\lambda_{c,T}^{0.02368}\left(\frac{k_{p,T}}{k_{y,T}}\right)^{-0.3028}+1.154\left(\frac{k_{p,T}}{k_{y,T}}\right)}{2.055+\lambda_{c,T}^{1.68}} \quad \text{for } \alpha>0 \tag{18}$$

$$\frac{b_{e1}}{b}=\frac{1}{3}(q_1\lambda_{c,T}^{q})\frac{0.8418\lambda_{c,T}^{0.02368}\left(\frac{k_{p,T}}{k_{y,T}}\right)^{-0.3028}+1.154\left(\frac{k_{p,T}}{k_{y,T}}\right)}{2.055+\lambda_{c,T}^{1.68}} \quad \text{for } \alpha=0 \tag{19}$$

$$\frac{b_{e2}}{b}=(1+\phi)\frac{b_{e1}}{b} \tag{20}$$

in which b_{e1} and b_{e2} are the effective widths shown in Fig. 25, q and q_1 are defined in Eqs. (16) and (17) respectively, and $\phi=1-\alpha$.

6. Comparisons with existing formulas

The effective width formulas proposed in this study for steel plates at ambient and elevated temperatures are validated by comparisons of the predicted ultimate strengths with those computed using expressions provided by Liang et al. [20], Couto et al. [25] and Quiel and Garlock [26]. For clamped steel plates at ambient temperature, Liang et al. [20] proposed formulas for calculating the ultimate strength of steel plates in CFST columns under stress gradients as follow:

$$\frac{\sigma_{1u}}{f_y}=c_1+c_2\left(\frac{b}{t}\right)+c_3\left(\frac{b}{t}\right)^2+c_4\left(\frac{b}{t}\right)^3 \tag{21}$$

where σ_{1u} is the ultimate strength corresponding to the maximum applied edge stress σ_1 and c_1, c_2, c_3 and c_4 are coefficients for every stress gradient ratio [20].

The expression for calculating the effective widths of steel plates at elevated temperatures presented by Quiel and Garlock [26] is written as

$$\frac{b_e}{b} = \frac{1.41}{\sqrt{\lambda_{c,T}\sqrt{k}}}\sqrt{\frac{k_{p,T}}{k_{y,T}}}\left(1-\frac{0.96}{k\lambda_{c,T}^{-0.5}}\right) < 1.0 \tag{22}$$

where k is taken as 4.0 for simply-supported plates and 7.0 for plates with two fixed unloaded edges and two simply-supported loaded edges [26].

Couto et al. [25] proposed an effective width formula for simply-supported steel plates at elevated temperatures as follow:

$$\frac{b_e}{b} = \frac{\left(\lambda_c + \alpha_T\right)^{\beta_T} - 0.055\left(3+\alpha\right)}{\left(\lambda_c + \alpha_T\right)^{2\beta_T}} \le 1.0 \tag{23}$$

where $\lambda_c = \sqrt{f_y / \sigma_{cr}}$ is the plate slenderness at ambient temperature, where σ_{cr} is the elastic local buckling of the plate at ambient temperature [5], and other parameters are defined as

$$\alpha_T = 0.9 - 0.315\frac{k_{0.2p,T}}{\varepsilon_T} \tag{24}$$

$$\beta_T = 2.3 - 1.1\frac{k_{0.2p,T}}{k_{y,T}} \tag{25}$$

$$\varepsilon_T = 0.85\sqrt{235/f_y} \tag{26}$$

The calculated ultimate strengths of thin steel plates under uniform edge compression at ambient temperature by using the proposed Eq. (15) are compared with those computed using formulas given by Liang et al. [20], and Quiel and Garlock [26] in Fig. 26. It can be observed that an excellent agreement between the strength curve computed by the proposed Eq. (15) and that given Liang et al. [20] is obtained. It should be noted that the effective width formulas for clamped steel plates proposed by Liang et al. [20] have been verified by experimental results on rectangular CFST columns. The strength curve predicted by the present study is conservative compared to the one given by Quiel and Garlock [26]. The reason for this is that the residual stresses are considered in the current model, but are not used in the model by Quiel and Garlock [26]. The comparison for elevated temperatures is depicted in Fig. 27. The post-local buckling strengths of steel plates predicted by the proposed formula are in good agreement with those given by Quiel and Garlock [26]. However, the results obtained by the formula of Couto et al. [25] are very conservative compared to the other two solutions as shown in Fig. 27. This is because the effective width formula given by Couto et al. [25] was developed for simply supported steel plates with initial geometric imperfections which were much larger than those incorporated in the finite element models in the present study.

7. Applications

The proposed effective width formulas for clamped steel plates at elevated temperatures can be used to account for local buckling effects on the ultimate axial loads of rectangular CFST short columns subjected to standard fire. A simple expression for determining the ultimate axial load of a CFST short column at elevated temperatures is proposed as

$$P_{u,cal} = A_{se} f_{y,T} + A_c f_{c,T} \tag{27}$$

where, $P_{u,cal}$ is the calculated ultimate axial load of the CFST short column, A_{se} is the effective cross-sectional area of the steel section computed using the proposed effective width formula Eq. 18, A_c is the concrete area of the section, and $f_{c,T}$ the compressive strength of concrete at elevated temperatures.

Dai and Lam [38] investigated the shape effects on the behavior of CFST short columns at elevated temperature using the commercial software package ABAQUS. Table 1 shows the geometric and material properties of square and rectangular CFST short columns provided by Dai and Lam [38]. The proposed effective width formulas and Eq. (27) were employed to calculate the ultimate axial loads of these columns and the results obtained are compared with those given by Dai and Lam [38] in Table 1. The reduction factors for the steel yielding strength and concrete at elevated temperatures given in Eurocode 3 [35] were adopted. As given in Table 1, the maximum temperature $(T_{\max})$ appeared at the corner of the steel cross-section, while the minimum temperature $(T_{\min})$ presented at the middle of the steel tube wall under consideration. It was assumed that the distribution of temperatures between the corner and the middle of the steel tube wall was linear. The concrete temperature was taken as 0.45 of the maximum temperature on the steel tube as suggested by Dai and Lam [38]. Local buckling of steel plates with *b/t* ratio greater than 20 was taken into account in the calculations of the ultimate axial loads. As demonstrated in Table 1, the calculated ultimate axial loads of CFST short columns at elevated temperatures are in good agreement with numerical results predicted using the finite element software ABAQUS. The mean ultimate axial loads computed by the proposed formulas are about 97 % and 94% of those reported by Dai and Lam [38] for the applied loads $(P_{u,app})$ of 500 kN and 600 kN, respectively.

The above comparative study demonstrates that the effective width formulas developed for steel

plates at elevated temperatures predict well the post-local buckling strengths of steel tube walls of CFST short columns exposed to fire. In addition, the assumed clamped boundary conditions for steel plates are able to simulate the boundary conditions of the steel tube walls of CFST columns at elevated temperatures.

8. Conclusions

The nonlinear critical local and post-local buckling behavior of thin steel plates under stress gradients in rectangular CFST columns at elevated temperatures has been investigated by using the finite element models developed. Geometric imperfections and residual stresses have been taken into account in the finite element models. The material stress-strain relationships for steels at elevated temperatures given in Eurocode 3 [35] have been adopted to simulate the material behavior. The critical local buckling and post-local buckling strength curves for clamped steel plates under compressive stress gradients at ambient and elevated temperatures have been determined from the finite element analysis results. Based on the numerical results obtained, design formulas for determining the critical local buckling and post-local buckling strengths of steel plates at ambient and elevated temperatures have been proposed. The effective width formulas have also been developed for clamped steel plates in rectangular CFST columns subjected to elevated temperatures.

The proposed formulas have been utilized to account for local buckling effects on the ultimate axial loads of CFST short columns exposed to fire. The results obtained are in good agreement with numerical solutions predicted by the finite element analysis software ABAQUS . The effective width models developed in this study can be incorporated in nonlinear analysis procedures to account for progressive post-local buckling effects on the behavior of thin-walled rectangular CFST columns exposed to fire. Furthermore, the proposed formulas can be used

directly in the design of CFST columns made of non-compact and slender steel sections at elevated temperatures.

References

[1] Schneider SP. Axially loaded concrete-filled steel tubes. Journal of Structural Engineering, ASCE 1998; 124(10): 1125-1138.

[2] Sakino K, Nakahara H, Morino S, Nishiyama I. Behavior of centrally loaded concrete-filled steel-tube short columns. Journal of Structural Engineering, ASCE 2004; 130(2): 180-188.

[3] Liang QQ, Patel VI, Hadi M N S. Biaxially loaded high-strength concrete-filled steel tubular slender beam-columns, Part I: Multiscale simulation. Journal of Constructional Steel Research 2012; 75:64-71.

[4] Dundu M. Column buckling tests of hot-rolled concrete filled square hollow sections of mild to high strength steel. Engineering Structures 2016; 127:73-85.

[5] Liang QQ. Analysis and design of steel and composite structures. Boca Raton and London: CRC Press, Taylor and Francis Group; 2014.

[6] Wang, YC. Steel and composite structures: Behaviour and design for fire safety, London and New York: Spon Press, 2002.

[7] Knobloch M. Local buckling behavior of steel sections subjected to fire. Fire Safety Science–Proceedings of the Ninth International Symposium, 2008: 1239-1254.

[8] Albero V, Espinos A, Romero ML, Hospitaler A, Bihina G, Renaud C. Proposal of a new method in EN1994-1-2 for the fire design of concrete filled steel tubular columns. Engineering Structures 2016; 128: 237-255.

[9] Espinos A, Romero ML, Hospitaler A. Simple calculation model for evaluating the fire resistance of unreinforced concrete filled tubular columns. Engineering Structures 2012; 42: 231-244.

[10] Rush DI, Bisby LA, Jowsey A, Lane B. Residual capacity of fire-exposed concrete-filled steel hollow section columns. Engineering Structures 2015; 100:550-563.

[11] Rodrigues JPC, Laim L. Fire response of restrained composite columns made with concrete filled hollow sections under different end-support conditions. Engineering Structures 2017; 141: 83-96.

[12] Rhodes J, Harvey JM. Effects of eccentricity of load or compression on the buckling and post-buckling behaviour of flat plates. International Journal of Mechanical Sciences 1971; 13(10):867–879.

[13] Rhodes J, Harvey JM, Fok WC. The load-carrying capacity of initially imperfect eccentrically loaded plates. International Journal of Mechanical Sciences 1975; 17(3):161–172.

[14] Usami T. Post-buckling of plates in compression and bending. Journal of Structural Division ASCE 1982; 108(3):591–609.

[15] Usami T. Effective width of locally buckled plates in compression and Bending. Journal of Structural Engineering ASCE 1993; 119(5):1358–1373.

[16] Shanmugam NE, Liew JYR, Lee SL. Thin-walled steel box columns under biaxial loading, Journal of Structural Engineering ASCE 1989; 115(11):2706-2726.

[17] Uy B, Bradford MA. Elastic local buckling of thin steel plates in composite steel-concrete members. Engineering Structures 1996; 18(3):193-200.

[18] Uy B, Bradford MA. Local buckling of thin steel plates in composite construction: Experimental and theoretical study. Proceedings of the Institution of Civil Engineers, Structures and Buildings 1995; 110:426-440.

[19] Uy B. Strength of concrete-filled steel box columns incorporating local buckling. Journal of Structural Engineering ASCE 2000; 126(3):341-352.

[20] Liang, QQ, Uy B, Liew, JYR. Local buckling of steel plates in concrete-filled thin-walled steel tubular beam-columns. Journal of Constructional Steel Research 2007; 63(3): 396-405.

[21] Liang QQ. Performance-based analysis of concrete-filled steel tubular beam–columns, Part I: Theory and algorithms. Journal of Constructional Steel Research 2009; 65:363–372.

[22] Liang QQ. Performance-based analysis of concrete-filled steel tubular beam–columns, Part II: Verification and applications. Journal of Constructional Steel Research 2009; 65:351–362.

[23] Ala-Outinen T, Myllymaki J. The local buckling of RHS members at elevated temperatures. VTT Research Notes 1672, Technical Research Centre of Finland (VTT), Espoo, Finaland, 1995.

[24] Heidarpour A, Bradford M.A. Local buckling and slenderness limits for flange outstands at elevated temperatures. Journal of Constructional Steel Research 2007; 63:591-598.

[25] Couto C, Real PV, Lopes N, Zhao B. Effective width method to account for the local buckling of steel thin plates at elevated temperatures. Thin-Walled Structures 2014; 84; 134-149.

[26] Quiel SE, Garlock MEM. Calculating the buckling strength of steel plates exposed to fire. Thin-Walled Structures 2010; 48; 684-695.

[27] ANSYS R 16.1. Academic, 2015.

[28] Feng M, Wang YC, Davies JM. A numerical imperfection sensitivity study of cold-formed thin-walled tubular steel columns at uniform elevated temperatures. Thin-walled Structures 2004; 42: 533-555.

[29] Abambres M, Quach WM. Residual stresses in steel members; a review of available analytical expressions. International Journal of Structural Integrity 2016; 7(1): 70-94.

[30] Chen, PS, Herman WA, Pense AW. Relaxation stresses in pressure vessels. Bulletin 302, February, Welding Research Council, New York, NY, 1985.

[31] Stout, RD. Postweld heat treatment of pressure vessels. Bulletin 302, February, Welding Research Council, New York, NY, 1985.

[32] Zhou RJ, Pense AW, Basehore ML, Lyons DH. A study of residual stress in pressure vessel steels. Bulletin 302, February, Welding Research Council, New York, NY, 1985.

[33] Tide RHR. Integrity of structural steel after exposure to fire. AISC Engineering Journal 1998; 35: 26- 38.

[34] Diesner RW. The effect of elevated temperature exposure on residual stresses. Sundstrand Aviation, 710285.

[35] Eurocode 3. Design of steel structures, Part 1.2: General rules-structural fire design, CEN, Brussels, Belgium, 2005.

[36] Von Karman T, Sechler EE, Donnell LH. The strength of thin plates in compression. Transactions of the American Society of Mechanical Engineers, 1932; 54:53-57.

[37] AISC. Steel construction manual, 13th edition. American Institute of Steel Construction; 2005.

[38] Dai XH, Lam D. Shape effect on the behaviour of axially loaded concrete filled steel tubular stub columns at elevated temperature. Journal of Constructional Steel Research, 2012; 73:117-127.

Figures and Tables

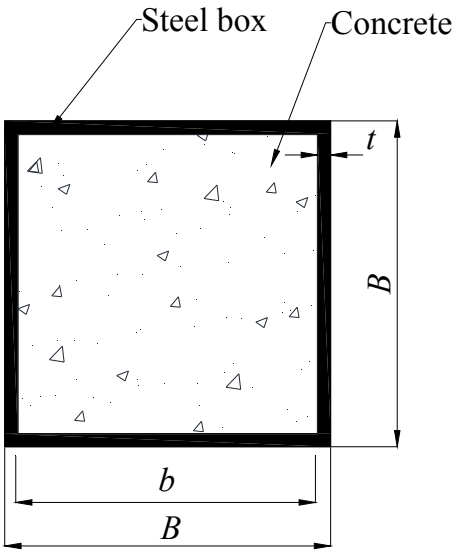

Fig. 1. Cross-section of square CFST beam-column.

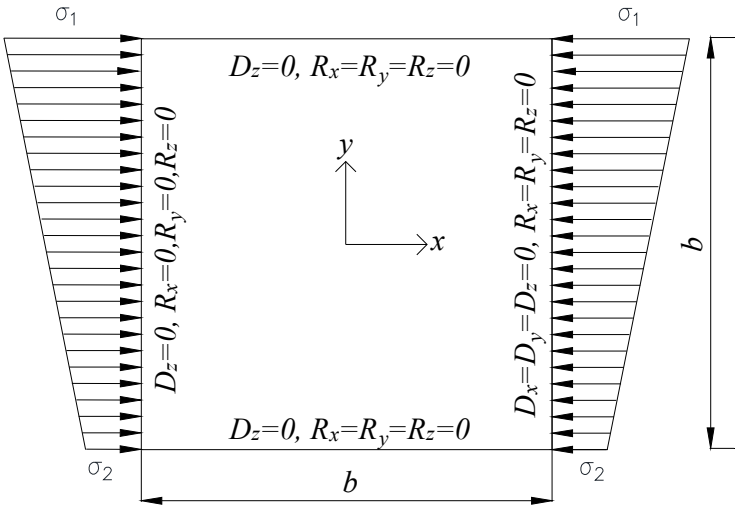

Fig. 2. Boundary conditions of clamped steel plate under compressive edge stresses.

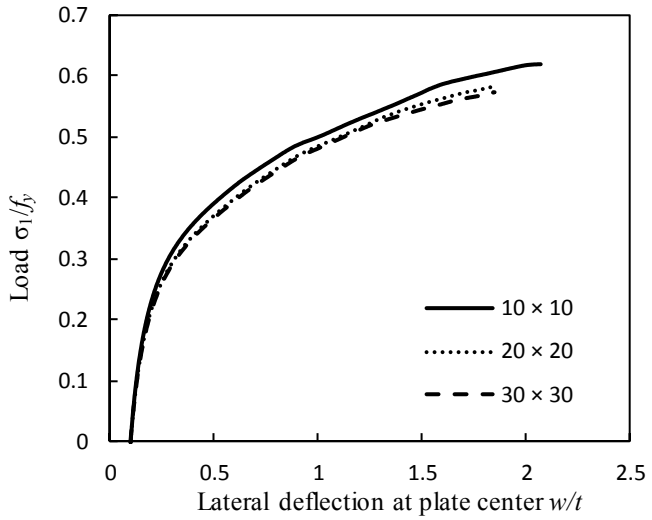

Fig. 3. Sensitivity analysis of element size on the load-deflection curves of square steel plate under uniform edge compression.

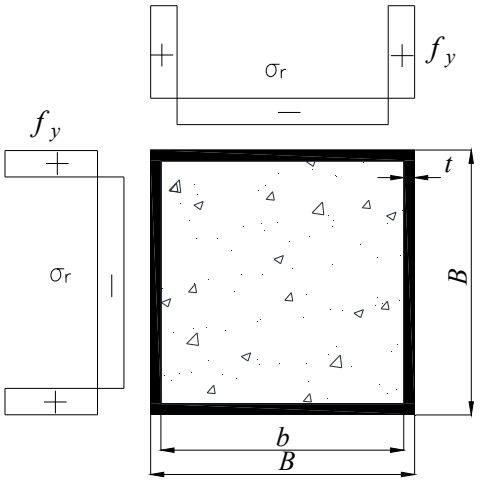

Fig. 4. Residual stress pattern in CFST beam-column.

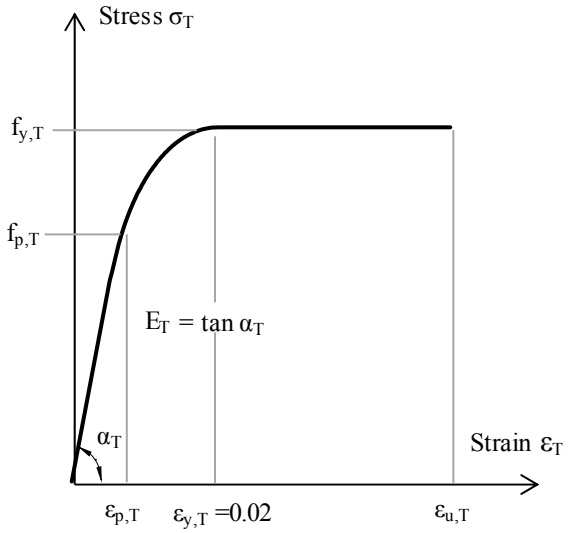

Fig. 5. Typical strain-stress curve of structural steel at elevated temperatures based on Eurocode 3 [35]

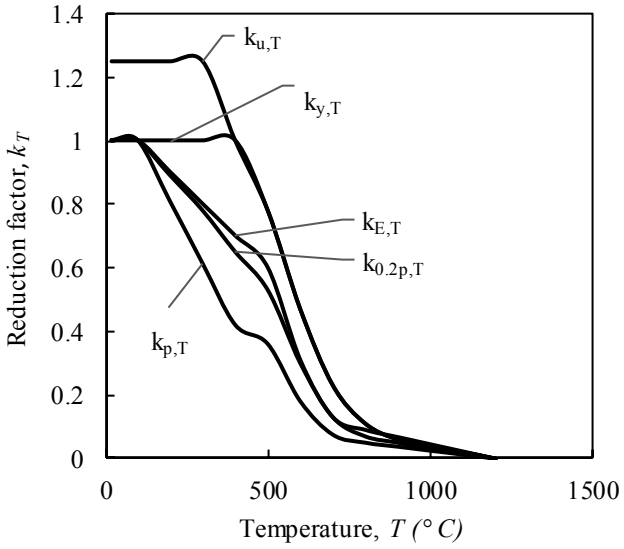

Fig. 6. Reduction factors k_T for stress-strain relationships allowing for strain-hardening of structural steel at elevated temperatures based on Eurocode 3 [35].

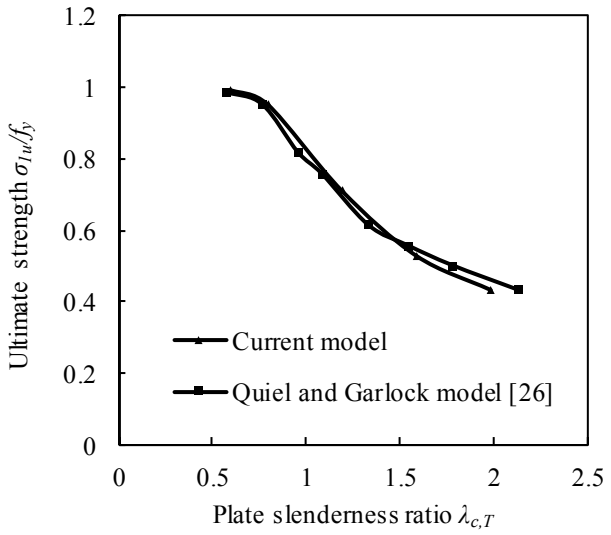

Fig. 7. Comparison of plate strength curves at ambient temperature predicted by the current model and Quiel and Garlock model [26].

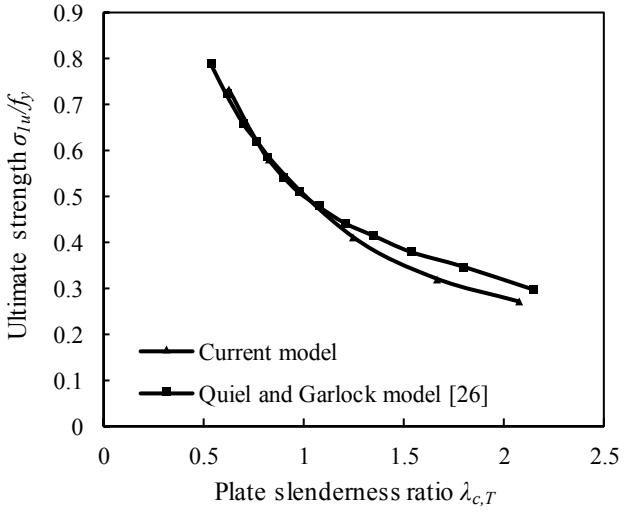

Fig. 8. Comparison of plate strength curves at temperate 700°C predicted by the current model and Quiel and Garlock model [26].

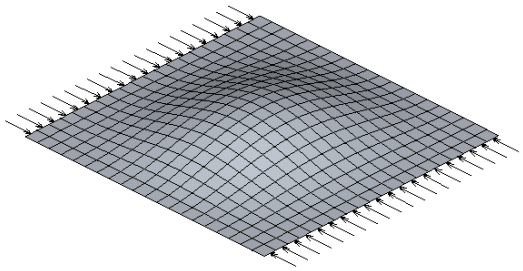

(a) Local buckling mode

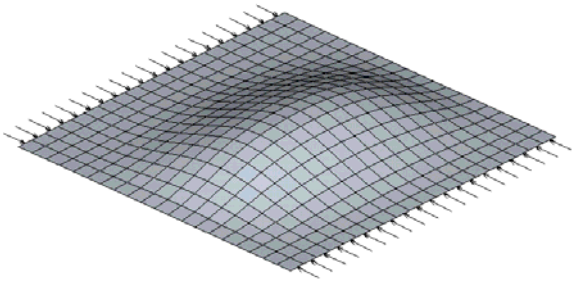

(b) Post-local buckling mode

Fig. 9. Buckling modes of clamped square steel plate under uniform edge compression at elevated temperatures.

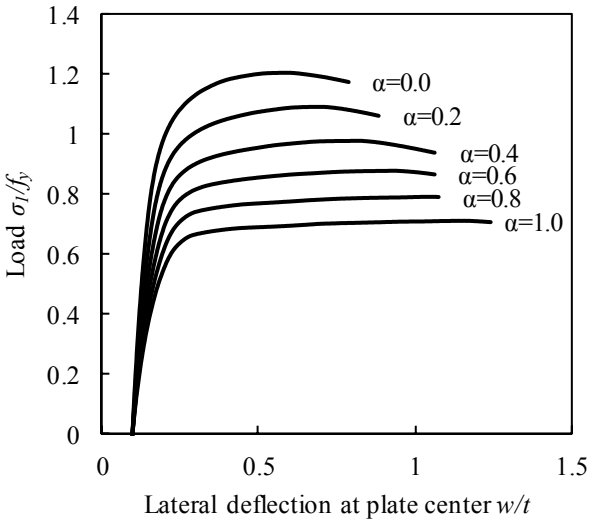

Fig. 10. Load-deflection curves for steel plates with b/t =70 under stress gradients at ambient temperature.

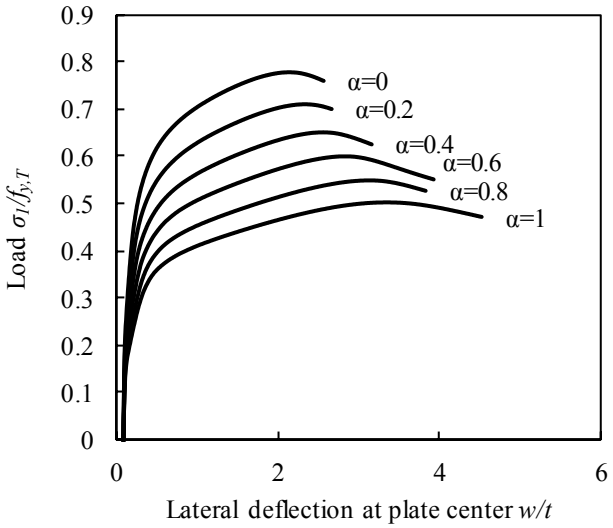

Fig.11. Load-deflection curves for steel plates with *b/t* =70 under stress gradients at temperature 600°C.

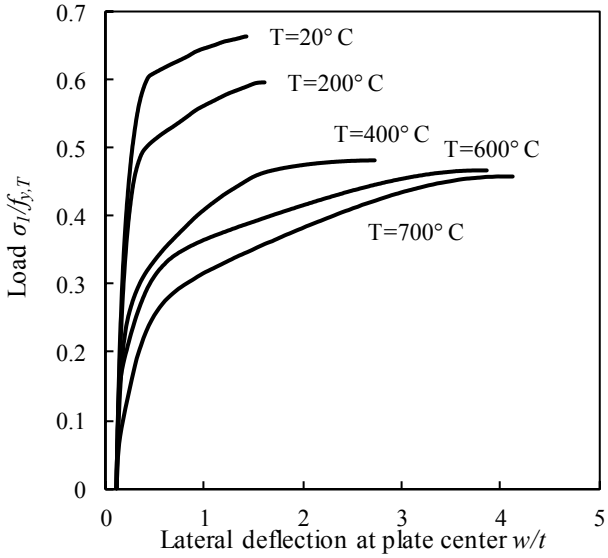

Fig. 12. Effect of temperatures on the load-deflection curves for steel plates with *b/t*=80 under uniform edge compression.

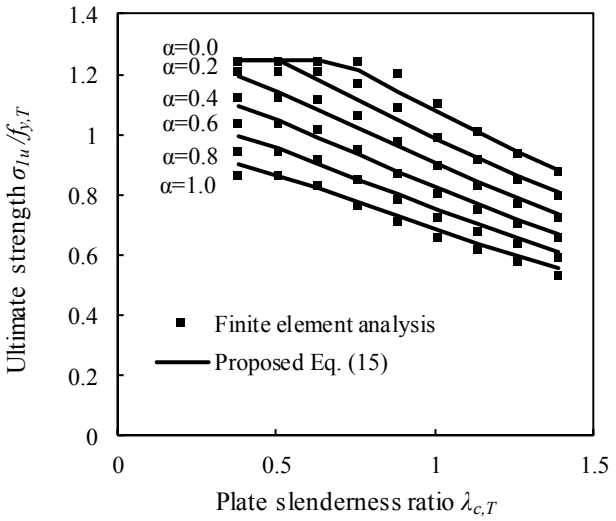

Fig. 13. Ultimate strengths of steel plates at ambient temperature.

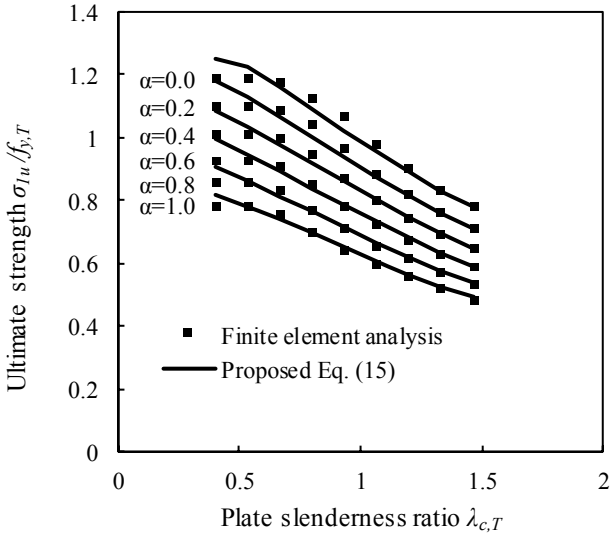

Fig. 14. Ultimate strengths of steel plates at temperature of 200°C.

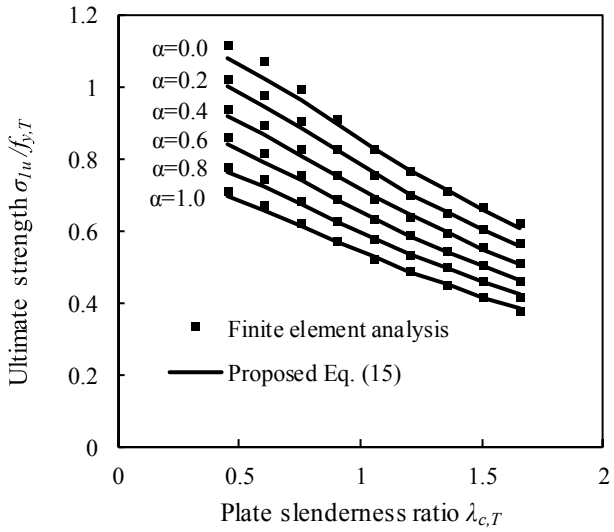

Fig. 15. Ultimate strengths of steel plates at temperature of 400°C.

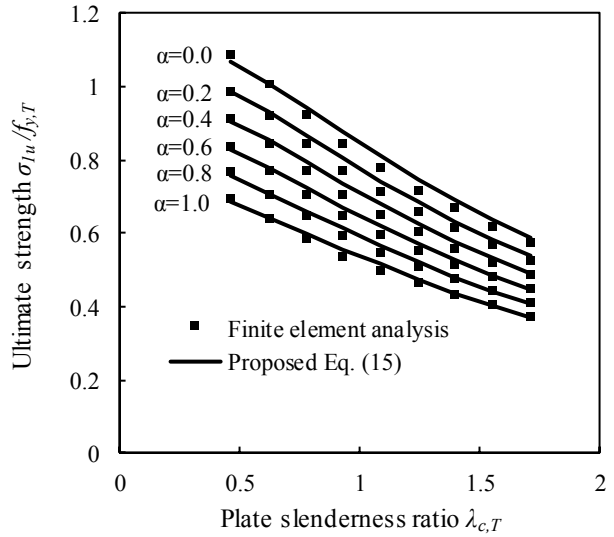

Fig. 16. Ultimate strengths of steel plates at temperature of 600°C.

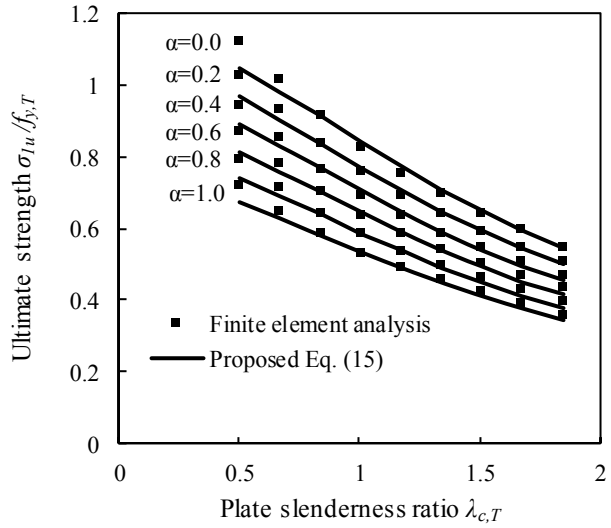

Fig. 17. Ultimate strengths of steel plates at temperature of 700°C.

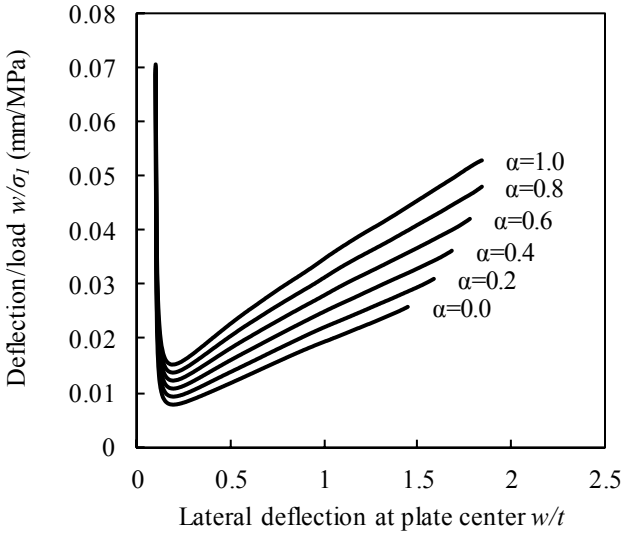

Fig. 18. Load-deflection curves for determining the critical local buckling strengths of steel plates with *b/t* ratio of 100 at ambient temperature.

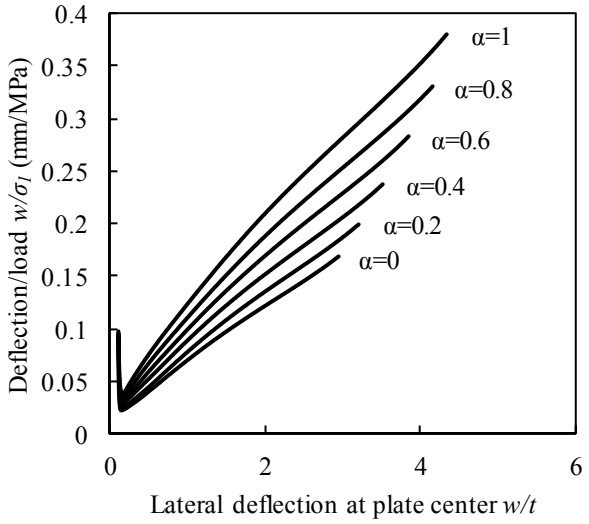

Fig. 19. Load-deflection curves for determining the critical local buckling strengths of steel plates with b/t ratio of 100 at temperature of 600° C.

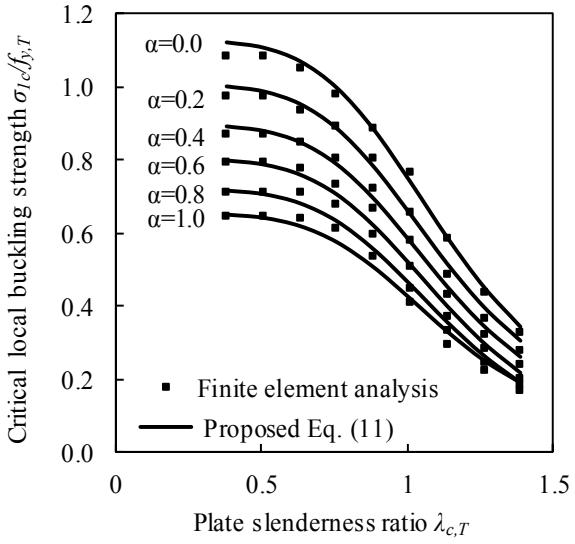

Fig. 20. Critical local buckling strengths of steel plates at ambient temperature.

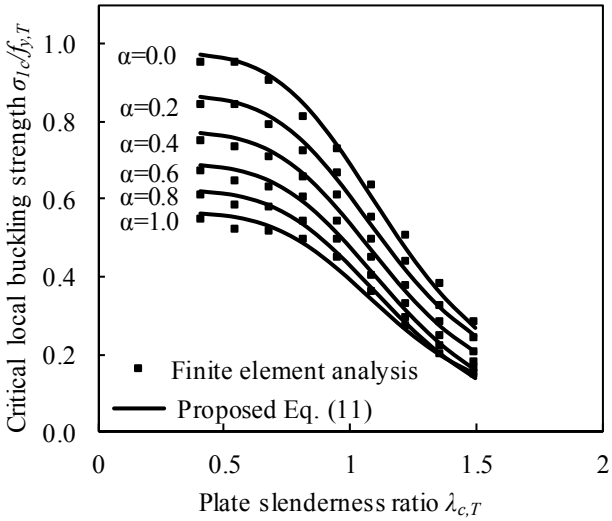

Fig. 21. Critical local buckling strengths of steel plates at temperature of 200°C.

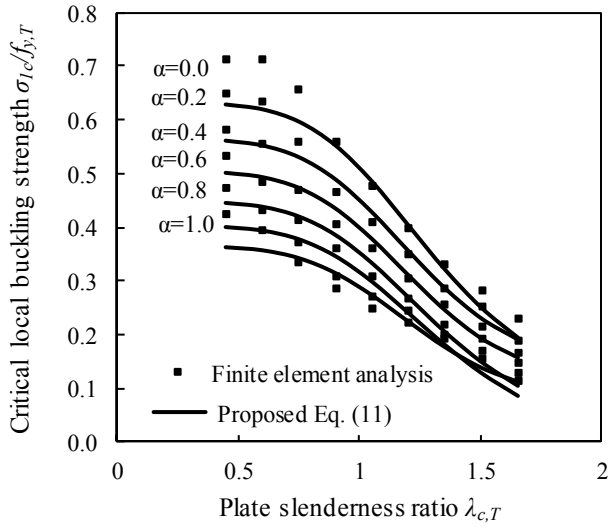

Fig. 22. Critical local buckling strengths of steel plates at temperature of 400°C.

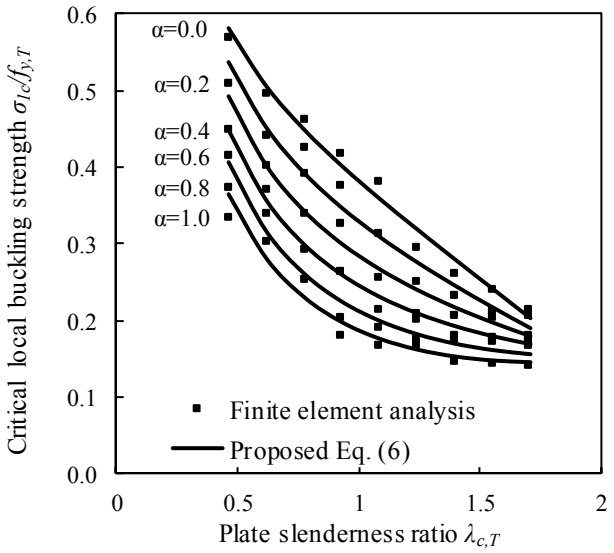

Fig. 23. Critical local buckling strengths of steel plates at temperature of 600°C.

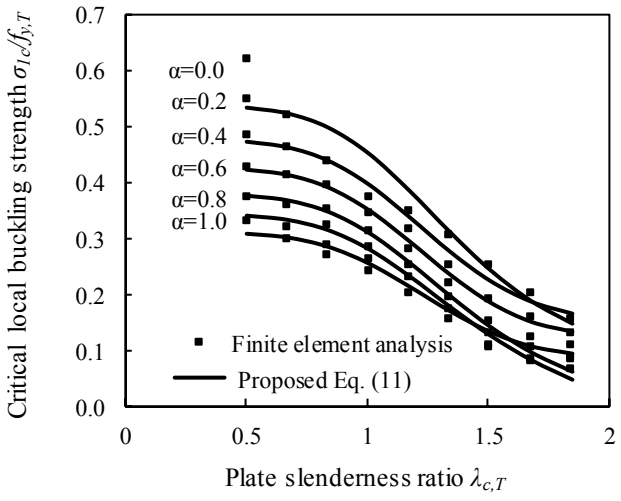

Fig. 24. Critical local buckling strengths of steel plates at temperature of 700°C.

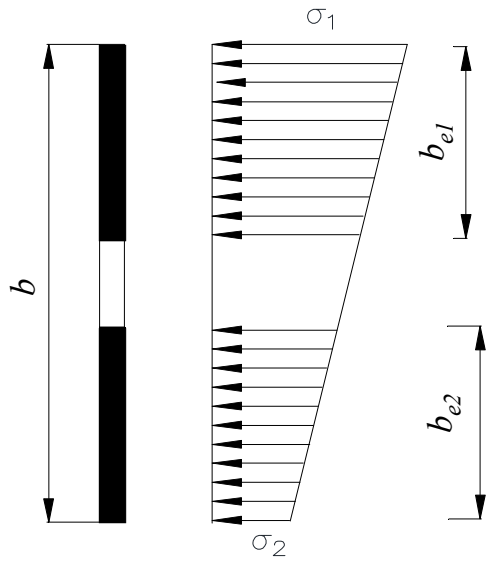

Fig. 25. Effective width of steel plate under stress gradient.

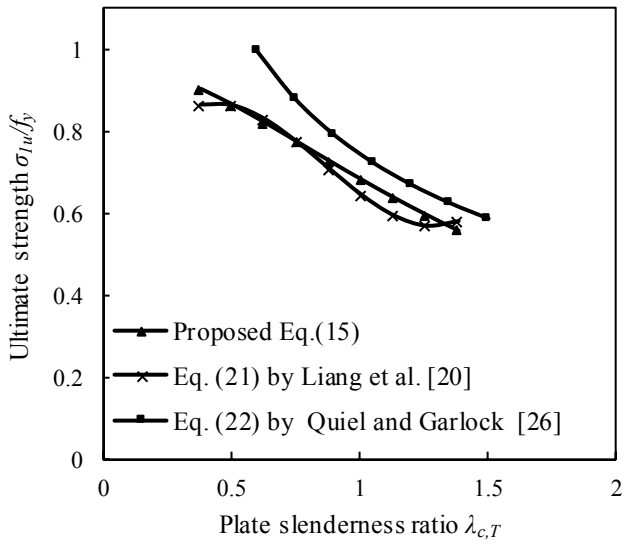

Fig. 26. Comparison of plate strength curves at ambient temperature predicted by the current proposed design formula with existing formulas.

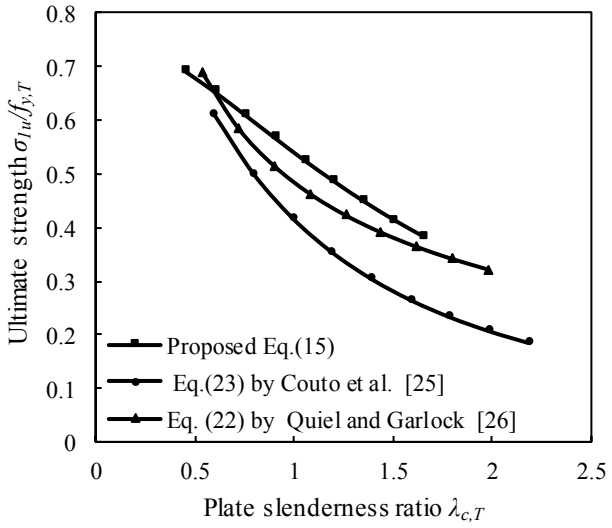

Fig. 27. Comparison of plate strength curves at temperature of 400°C predicted by the current proposed design formula with those given by Couto et al. [25] Quiel and Garlock [26]

Table1 Ultimate axial loads of rectangular CFST short columns at elevated temperatures.

Specimen	Dimensions	$P_{u,app}$ = 500 kN				$P_{u,app}$ = 600 kN			
	$B\times D\times t$ (mm)	$T_{\max}$ (°C)	$T_{\min}$ (°C)	$P_{u,cal}$ (kN)	$\frac{P_{u,cal}}{P_{u,app}}$	$T_{\max}$ (°C)	$T_{\min}$ (°C)	$P_{u,cal}$ (kN)	$\frac{P_{u,cal}}{P_{u,app}}$
SHS	123×123×5	690	652	490.1	0.98	648	607	559.7	0.93
SHS1	118.9×118.9×5	712	678	431.7	0.86	644	605	534.6	0.89
SHS2	125.9×125.9×5	700	661	494.3	0.99	675	634	536.8	0.89
RHS	84.5×169×5	695	633	499	1.00	645	579	595.4	0.99
RHS1	79.3×158.5×5	687	628	460.4	0.92	632	570	560.1	0.93
RHS2	89.5×179×5	716	655	517.7	1.04	676	610	588.2	0.98
Mean					0.97				0.94